Iranian Food Science and Technology Research Journal
Vol. 12, No. 6, Feb. Mrch. 2017, p. 758-766

نشریه پژوهشهای علوم و صنایع غذایی ایران
جلد 12، شماره 6، بهمن - اسفند 1395، ص. 766-758

Experimental and modeling investigation of mass transfer during infrared drying of Quince

M. A. Mehrnia [1*], A. Bashti[2], F. Salehi[3]

Received: 2017.01.10
Accepted: 2017.05.08

Abstract

In this research, an experimental and modeling study on mass transfer analysis during infrared drying of quince was undertaken. In the experimental part, the effects of various drying conditions in terms of infrared radiation power (150-375 W) and distance (5-15 cm) on drying characteristics of quince were investigated. Both the infrared power and distance influenced the drying time of quince slices. Moisture ratios were fitted to 8 different mathematical models using nonlinear regression analysis. The regression results showed that the logarithmic model satisfactorily described the drying behavior of quince slices with highest R value and lowest SE values. The effective moisture diffusivity increases as power increases and range between 1.15 and 3.72 $\times 10^{-8}$ m^2/s. The rise in infrared power has a negative effect on the ΔE and with increasing in infrared radiation power it was increased. Chroma and hue values were in ranges between 43.28 and 46.99, 80.82° and 86.14°, respectively.

Keywords: Effective moisture diffusivity, Image processing; Infrared dryer; Quince.

Introduction

Fruits have very short shelf-life due to high moisture content (above 82% by weight), and it is necessary to use various preservation methods to increase its shelf life (Cassano *et al.*, 2006). Drying appears to be a potential food preservation option to extend their storage/shelf-life. Maskan (2001) studied to comparison of the microwave, hot air and hot air-microwave drying methods for the processing of kiwifruits in respect to drying, shrinkage and rehydration characteristics obtained by the three drying techniques. Chen *et al*. (2001) established the drying kinetics parameters through the experiments performed on pulped kiwifruit flesh spread onto a shallow metal tray (forming a layer) to simulate the process of making fruit leather.

Quince, (*Cydonia oblonga*) from Rosaceae family, is a tree cultivated as a medicinal and nutritional plant in the Middle East, South Africa, and central Europe (Hemmati *et al*., 2012). They are used to make jam, marmalade, jelly and quince pudding (de Escalada Pla *et al*., 2010). Drying is one of the important preservation methods employed for storage of quince. Drying kinetics of quince slices was investigated by Kaya *et al*. (2007) and the effect of drying method on bulk density, substance density, porosity, and shrinkage of quinces at various moisture contents was studied by Koç *et al*. (2008).

One of the ways to shorten the drying time is to supply heat by infrared radiation. Its efficiency is between 80% and 90%, the emitted radiation is in narrow wavelength range and they are miniaturized (Sakai and Hanzawa, 1994; Sandu, 1986). Advantages of infrared radiation over convective heating include high heat transfer coefficients, short process times and low energy costs (Ratti and Mujumdar, 1995). Comparison of infrared drying with convective drying of apple showed that time of the process can be shortened by up to 50% when heating is done with infrared energy (Nowak and Lewicki, 2004). The combination of infrared with hot air provides

1. Assistant professor, Department of Food Science & Technology, Shoushtsar Branch, Islamic azad university, shoushtar ,Iran
2. Assistant professor , Department of Chemistry, Shoushtar Branch, Islamic Azad university, Shoushtar, Iran.
3. Assistant professor , Department of Food Science and Technology, Bu-Ali Sina University, Hamedan, Iran.
Corresponding Author Email: mamehrnia@yahoo.com
DOI: 10.22067/ifstrj.v12i6.61732

the synergistic effect, resulting in an efficient drying process. Energy and quality aspects were studied during combined far infrared and convective drying of barley (Afzal *et al*., 1999).

Infrared drying was applied before or after freeze-drying of shiitake mushroom to shorten the drying time, enhance the rehydration, and for better preservation of the aroma compounds and color (Wang *et al*. (2015). The reported results showed that the combination of freeze-drying (for 4h) followed by infrared drying saves 48% time compared to freeze-drying while keeping the product quality at an acceptable level. The application of infrared drying also helps produce a more porous microstructure in dried shiitake mushrooms.

Pan *et al*. (2008) used sequential infrared and freeze-drying (SIRFD) to produce high-quality dried fruits at reduced cost. The products dried using SIRFD had better color, higher crispness, higher shrinkage but poor rehydration propensity compared to those produced by using regular freeze-drying (Pan *et al*., 2008).

Infrared drying method, when properly applied, can be used for achieving a high-quality product. There for, the aim of the present work was to investigate infrared drying characteristics of quince slices in respect to drying kinetics, moisture diffusivity and color changes of the dried products.

Materials and methods

Infrared drying

Quinces used in this study were purchased from a local market and they had no external defects. The initial moisture content of quinces was found to be 84% ± 1.05 (wet basis). Prior to drying, samples were taken out of storage, peeled with a sharp vegetable peeler, and cut into 5 mm thick slices with a steel cutter.

The quince slices were dried in an infrared dryer (Infrared radiation lamp (NIR), Noor, Iran). The effect of infrared radiation power (at three levels 150, 250 and 375 W) and distance (at three levels 5, 10 and 15 cm) on the drying kinetics and characteristics of quince slice were investigated. Then the dried samples stored in an air-tight packet till the experiments.

Weight loss of samples was recorded by using a digital balance (Digital balance, Lutron GM-300p, Taiwan), with a sensitivity of ±0.01 g. The initial moisture content of the samples was obtained according to the AOAC method no. 934.06 (AOAC 1990). Experiments were carried out in triplicate and an arithmetic average was taken for data processing.

Drying kinetics

The experimental moisture content data were nondimensionlized using the equation 1:

$$MR = \frac{M_t - M_e}{M_0 - M_e} \quad (1)$$

Where MR is the dimensionless moisture ratio, M_t, M_0 and M_e are moisture content at any time, initial moisture content and equilibrium moisture content (kg water/kg dry matter), respectively. $(M_t–M_e)/(M_0–M_e)$ was simplified to M_t/M_0 as the relative humidity of drying air continuously fluctuated during drying experiments (Ceylan *et al*., 2007; Doymaz, 2011).

Selected thin-layer drying models (Approximation of diffusion, Page, Newton, Midilli, Logarithmic, Verma, Two term, Quadratic) were fitted to the drying curves (MR versus time) (Akpinar and Bicer, 2005; Doymaz, 2011). A nonlinear estimation package (Curve Expert, Version 1.34) was used to estimate the coefficients of the given models. The two criteria of statistic analysis have been used to evaluate the adjustment of the experimental data to the different models, r (correlation coefficient) and SE (standard error). A good fitting between the experimental data and the correlations is obtained when there is a combination of the high r value and the values of SE, which should be as low as possible (Doymaz, 2011).

Calculation of Moisture Diffusivity

In most of drying studies, diffusion is generally accepted to be the main mechanism during the transport of moisture to the surface to be evaporated (Doymaz, 2011). Fick's second law of diffusion has been widely used

to describe the drying process during the falling rate period for most food materials (Sacilik, 2007). The solution of diffusion model, considering negligible external resistance, in terms of average moisture content, negligible shrinkage, constant diffusion coefficients and temperature, is presented for slab geometry as follows (Doymaz, 2011):

$$MR = \frac{8}{\pi^2}\sum_{n=0}^{\infty}\frac{1}{(2n+1)^2}\exp(-(2n+1)^2\frac{\pi^2 D_{eff}t}{4L^2}) \quad (2)$$

Where MR is the moisture ratio (dimensionless); t is the drying time (s), D_{eff} is the effective diffusivity (m^2/s); and L is the half slab thickness of the slices (m). For long drying periods, equation 2 can be further simplified to only the first term of the series. Equation 2 thus simplifies to:

$$MR = \frac{8}{\pi^2}\exp\left[\frac{-\pi^2 D_{eff}t}{4L^2}\right] \quad (3)$$

The effective diffusivity was calculated through equation 3 by using the method of slopes. The effective diffusivities are typically determined by plotting experimental drying data in terms of lnMR versus time (as given in equation 3). From equation 3, a plot of lnMR versus time gives a straight line with a slope (K) of:

$$K = \frac{\pi^2 D_{eff}}{4L^2} \quad (4)$$

Color measurement

In order to investigate the effect of drying condition on the color changes of dried quince, a computer vision system was applied. Sample illumination was achieved with HP Scanner (Hp-G3110). Since the computer vision system perceived color as RGB signals, which is device-dependent, the taken images were converted into $L^*a^*b^*$ units to ensure color reproducibility. In the L*a*b* space, the color perception is uniform, and therefore, the difference between two colors corresponds approximately to the color difference perceived by the human eye. L^* (lightness/darkness that ranges from 0 to 100), a^*(redness/greenness that ranges from -120 to 120) and b^* (yellowness/blueness that ranges from -120 to 120) were measured. In this study, the image analysis of dried quince was performed using Image J software version 1.42e, USA.

The hue angle (°), hue = arctg (b^*/a^*), expresses the colour nuance and values are defined as follows: red-purple: 0°, yellow: 90°, bluish-green: 180°, and blue: 270°. Hue angle (H) of the films was calculated as follows (Bhat *et al.*, 2013):

$H = \tan^{-1}(b^*/a^*)$ when $a^* > 0$ and $b^* > 0$

$H = 180° + \tan^{-1}(b^*/a^*)$ when $a^* < 0$

$H = 360° + \tan^{-1}(b^*/a^*)$ when $a^* > 0$ and $b^* < 0$

The calculation of color changes (ΔE) for total color difference and C^* (Chroma) for saturation were made with the following equations (Liu *et al*., 2010):

$$\Delta E = \sqrt{(\Delta L^*)^2 + (\Delta a^*)^2 + (\Delta b^*)^2} \quad (5)$$

$$C^* = \sqrt{(a^*)^2 + (b^*)^2} \quad (6)$$

Results and discussion

Drying time

During drying, radiation properties of the material are changing due to decreasing water content. As a consequence, its reflectivity increases and the absorptivity decrease. Generally, solid materials absorb infrared radiation in a thin surface layer (Lampinen *et al*., 1991).

The effects of infrared power and distance on the moisture content of quince slices are shown in figures 1 and 2. As expected, the moisture content was decreased by increasing the power because of the increased temperature and heat transfer gradient between the air and samples. The drying times of quince samples were 18, 29 and 44 min at 150, 250 and 375 W, respectively (10 cm). In conclusion, experimental results showed that the infrared power has a significant effect on the evolution of moisture content.

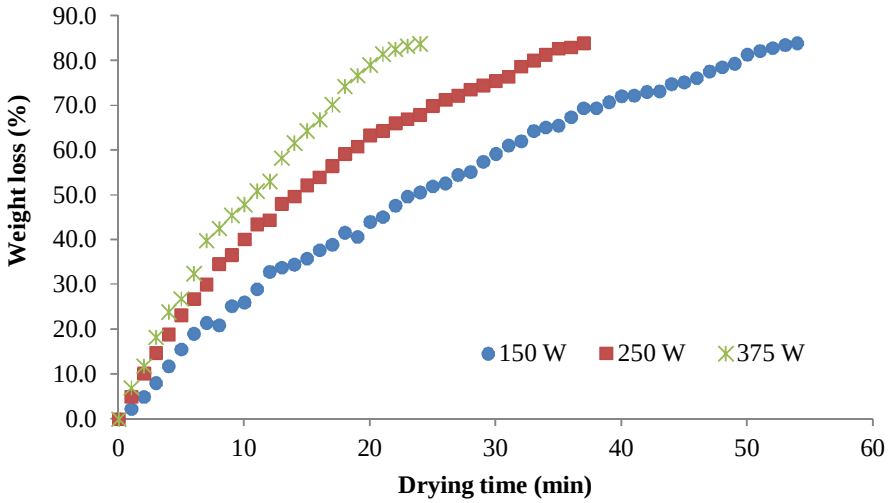

Figure 1. Variations of moisture content with drying time of quince slices at different infrared power.

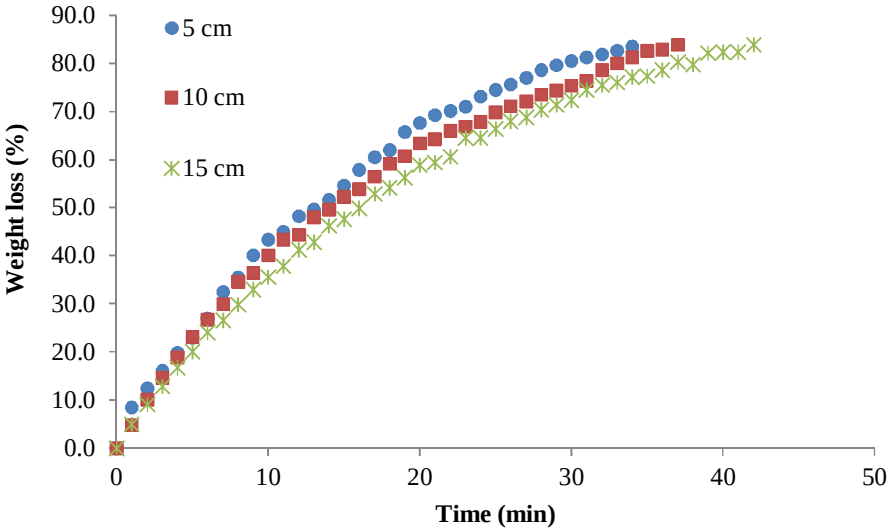

Figure 2. Variations of moisture content with drying time of quince slices at different distance.

Hence, drying of thin layers seems to be more efficient at far-infrared radiation (FIR, 25–100 μm), while drying of thicker bodies should give better results at near-infrared radiation (NIR, 0.75–3.00 μm) (Nowak and Lewicki, 2004). The drying time reduced from 31 to 25 min when the distance was increased from 15 to 5 cm (250 W).

Fitting of the Drying Curves

Different mathematical models were fitted to the drying data and among them; the Logarithmic model showed the highest r and the lowest SE values. Estimated parameters and statistical data obtained for this model are shown in Table 1. In all the cases, the r values for the models were greater than 0.997, indicating a good fit. It can be seen that there was a very good agreement between the experimental and predicted moisture ratio values, which are closely banding around at a 45° straight line.

Table 1. Curve-fitting coefficients of the Logarithmic model.

Power (W)	Distance (cm)	a	k	c	r	SE
150	5	1.309	0.026	-0.355	0.999	0.014
250	10	1.335	0.024	-0.353	0.999	0.015
375	15	1.345	0.020	-0.376	0.999	0.013
150	5	1.189	0.053	-0.205	0.999	0.011
250	10	1.145	0.051	-0.158	0.999	0.009
375	15	1.172	0.044	-0.181	0.999	0.006
150	5	3.631	0.020	-2.604	0.997	0.025
250	10	1.469	0.049	-0.481	0.999	0.015
375	15	1.322	0.053	-0.304	0.999	0.010

Moisture Diffusivity

The effective diffusivities are determined by plotting experimental drying data in terms of lnMR versus time. The effects of infrared radiation power and distance on the lnMR are shown in Figures 3 and 4. The D_{eff} values lie within in general range of 10^{-11} to 10^{-9} m^2/s for food materials (Rizvi, 1986). The values of D_{eff} at different condition drying of quince slice obtained by using Eq. (4) and estimated values are shown in Table 2. The effective diffusivity values of quince slices were ranged from 1.00 and 3.72 $\times 10^{-8}$ m^2/s. Effective diffusivity values increased with increasing infrared radiation power because of the rapid movement of water at high temperatures (Doymaz, 2011).

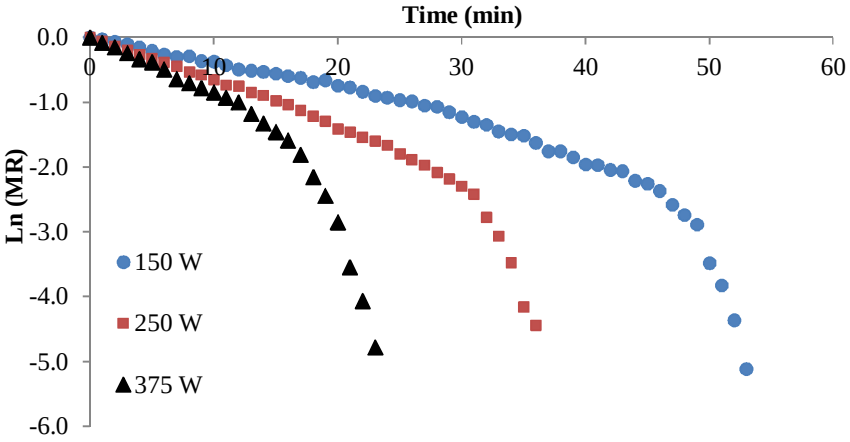

Figure 3. Effect of infrared power on the Ln(MR) during drying of quince slices.

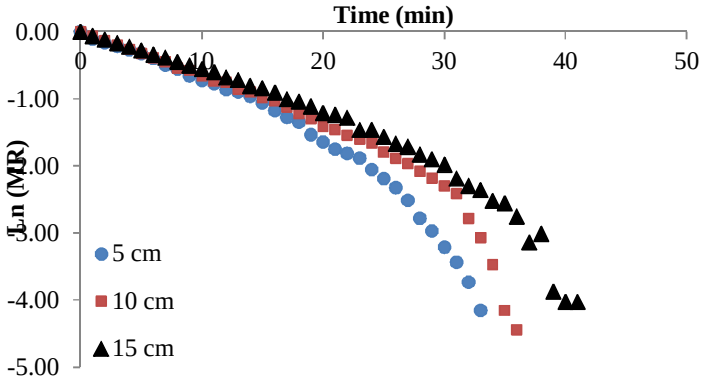

Figure 4. Effect of infrared source distance on the Ln(MR) during drying of quince slices.

Table 2. Values of effective moisture diffusivity of quince slice obtained from drying experiments.

Power (W)	Distance (cm)	Effective diffusivity (m^2/s)	r
150	5	1.15×10^{-8}	0.928
250	10	1.08×10^{-8}	0.918
375	15	1.00×10^{-8}	0.902
150	5	1.83×10^{-8}	0.969
250	10	1.62×10^{-8}	0.945
375	15	1.43×10^{-8}	0.963
150	5	3.72×10^{-8}	0.886
250	10	2.82×10^{-8}	0.920
375	15	2.30×10^{-8}	0.933

The values of D_{eff} are comparable with the reported values of 0.85 to 1.75 $\times10^{-10}$ m^2/s for hull-less seed pumpkin at 40–60°C (Sacilik, 2007), 0.46–3.45 $\times10^{-10}$ m^2/s mentioned for drying carrot in the temperature range of 60–90°C (Zielinska and Markowski, 2007), 3.0 to 17.12 $\times10^{-10}$ m^2/s for kiwifruit at 30–90°C (Simal *et al*., 2005), 3.2 to 11.2 $\times$ 10^{-9} m^2/s for red bell pepper at 50–80°C (Vega *et al*., 2007), 2.52 to 13.0×10^{-10} m^2/s for curd at 45–50°C (Shiby and Mishra, 2007), and 4.27 to 13.0×10^{-10} m^2/s okra at 50–70°C (Doymaz, 2005). These values are consistent with the present estimated D_{eff} values for quince slices

Color measurement

The fresh quince exhibited a light yellow color, with L*, a* and b* equal to 89.13, -2.763 and 54.962, respectively. The results of color measurement of dried quince slices at different conditions are presented in Table 3. The infrared radiation power was found to have a significant effect on the colour of quince slices. The rise in power has a negative effect on the ΔE and with increasing in infrared radiation power from 250 to 375 W, it was increased from 15.34 to 24.84, respectively. Therdthai and Zhou (2009) reported that high temperature during drying of mint leaves could lead to increase ΔE values (Therdthai and Zhou, 2009).

As shown in table 3, the L^* values varied from 65.74 to 79.61 at different drying condition. Chroma and hue values were in ranges between 43.28 and 46.99, 80.82° and 86.14°, respectively. The chroma value indicates the degree of saturation of colour and is proportional to the strength of the colour. The changes in Hue angle values were not significant compared to drying processes.

Table 3. Comparison the effect of different drying methods on color change of quince slices.

Power (W)	Distance (cm)	a^*	b^*	L^*	ΔE	C*	Hue value (°)
150	5	3.23±1.37	29.40±14.26	45.54±3.03	15.18	45.65	85.94
250	10	3.05±1.30	35.85±12.84	45.21±2.89	16.40	45.32	86.14
375	15	3.06±1.34	34.69±13.81	45.5±2.76	18.05	45.16	86.11
150	5	4.43±2.33	32.73±13.98	46.78±5.49	14.46	46.99	84.59
250	10	4.16±1.57	30.05±12.57	46.56±2.79	15.05	46.75	84.89
375	15	4.05±1.59	31.93±13.33	46.38±2.85	16.51	46.56	85.02
150	5	5.41±2.02	28.45±11.68	44.36±4.89	20.23	44.69	83.04
250	10	6.94±1.95	31.55±14.02	42.93±3.22	26.20	43.48	80.82
375	15	6.87±2.22	33.52±14.21	42.73±4.39	28.10	43.28	80.87

Conclusions

An infrared system was used for drying of quince. A drying system was fitted with near-infrared (NIR) heaters for radiative heating. The drying times of quince samples were 18, 29 and 44 min at 150, 250 and 375 W, respectively. The drying times was reduced when the distance of sample from infrared source was decreased. The drying characteristics were satisfactorily described by Logarithmic model with the latter providing the best representation of the experimental data. Values for the effective moisture diffusivity of quince samples were obtained in the range of 1.00 and 3.72 $\times10^{-8}$ m^2/s. The present study also verified that the color of

quince was influenced by the drying process. The rise in power has a negative effect on the ΔE and with increasing in infrared radiation power from 250 to 375 W, it was increased from 15.34 to 24.84, respectively. The changes in Hue angle values were not significant compared to drying processes.

References

Afzal, T., Abe, T., Hikida, Y., 1999. Energy and quality aspects during combined FIR-convection drying of barley. *Journal of Food Engineering*, 42(4), 177-182.

Akpinar, E.K., Bicer, Y., 2005. Modelling of the drying of eggplants in thin-layers. I*nternational Journal of Food Science & Technology*, 40(3), 273-281.

Bhat, R., Abdullah, N., Din, R.H., Tay, G.-S., 2013. Producing novel sago starch based food packaging films by incorporating lignin isolated from oil palm black liquor waste. *Journal of Food Engineering*, 119(4), 707-713.

Cassano, A., Figoli, A., Tagarelli, A., Sindona, G., Drioli, E., 2006. Integrated membrane process for the production of highly nutritional kiwifruit juice. *Desalination*, 189(1), 21-30.

Ceylan, I., Aktaş, M., Doğan, H., 2007. Mathematical modeling of drying characteristics of tropical fruits. *Applied Thermal Engineering*, 27(11), 1931-1936.

Chen, X., Pirini, W., Ozilgen, M., 2001. The reaction engineering approach to modelling drying of thin layer of pulped Kiwifruit flesh under conditions of small Biot numbers. *Chemical Engineering and Processing: Process Intensificat*ion, 40(4), 311-320.

de Escalada Pla, M.F., Uribe, M., Fissore, E.N., Gerschenson, L.N., Rojas, A.M., 2010. Influence of the isolation procedure on the characteristics of fiber-rich products obtained from quince wastes. *Journal of Food Engineering*, 96(2), 239-248.

Doymaz, I., 2011. Drying of eggplant slices in thin layers at different air temperatures. *Journal of Food* P*rocessing and Preservation*, 35(2), 280-289.

Doymaz, İ., 2005. Drying characteristics and kinetics of okra. Journal of Food Engineering, 69(3), 275-279.

Hemmati, A.A., Kalantari, H., Jalali, A., Rezai, S., Zadeh, H.H., 2012. Healing effect of quince seed mucilage on T-2 toxin-induced dermal toxicity in rabbit. *Experimental and Toxicologic Pathology*, 64(3), 181-186.

Kaya, A., Aydin, O., Demirtas, C., Akgün, M., 2007. An experimental study on the drying kinetics of quince. *Desalination*, 212(1–3), 328-343.

Koç, B., Eren, İ., Kaymak Ertekin, F., 2008. Modelling bulk density, porosity and shrinkage of quince during drying: The effect of drying method. Journal of Food Engineering, 85(3), 340-349.

Lampinen, M.J., Ojala, K.T., Koski, E., 1991. Modeling and measurements of infrared dryers for coated paper. *Drying Technology*, 9(4), 973-1017.

Liu, F., Cao, X., Wang, H., Liao, X., 2010. Changes of tomato powder qualities during storage. *Powder Technology*, 204(1), 159-166.

Maskan, M., 2001. Drying, shrinkage and rehydration characteristics of kiwifruits during hot air and microwave drying. J*ournal of Food Engineering*, 48(2), 177-182.

Nowak, D., Lewicki, P.P., 2004. Infrared drying of apple slices. *Innovative Food Science & Emerging Technologies*, 5(3), 353-360.

Pan, Z., Shih, C., McHugh, T.H., Hirschberg, E., 2008. Study of banana dehydration using sequential infrared radiation heating and freeze-drying. *LWT-Food Science and Technology*, 41(10), 1944-1951.

Ratti, C., Mujumdar, A., 1995. Infrared drying. Handbook of Industrial Drying, Ed. Mujumdar, A. S., Second edition, New York, NY, *Marcel Dekker* Inc., 1, 567-588.

Rizvi, S.S., 1986. Thermodynamic properties of foods in dehydration, Engineering properties of foods. CRC Press, pp. 239-251.

Sacilik, K., 2007. Effect of drying methods on thin-layer drying characteristics of hull-less seed pumpkin (*Cucurbita pepo* L.). *Journal of Food Engineering*, 79(1), 23-30.

Sakai, N., Hanzawa, T., 1994. Applications and advances in far-infrared heating in Japan. Trends in Food Science & Technology, (11), 357-362.

Sandu, C., 1986. Infrared radiative drying in food engineering: a process analysis. *Biotechnology Progress*,

2(3), 109-119.
Shiby, V., Mishra, H., 2007. Thin layer modelling of recirculatory convective air drying of curd (*Indian yoghurt*). *Food and Bioproducts Processing*, 85(3), 193-201.
Simal, S., Femenia, A., Garau, M., Rosselló, C., 2005. Use of exponential, Page's and diffusional models to simulate the drying kinetics of kiwi fruit. *Journal of Food Engineering*, 66(3), 323-328.
Therdthai, N., Zhou, W., 2009. Characterization of microwave vacuum drying and hot air drying of mint leaves (Mentha cordifolia Opiz ex Fresen). *Journal of Food Engineering*, 91(3), 482-489.
Vega, A., Fito, P., Andrés, A., Lemus, R., 2007. Mathematical modeling of hot-air drying kinetics of red bell pepper (var. *Lamuyo*). *Journal of Food Engineering*, 79(4), 1460-1466.
Wang, H.-c., Zhang, M., Adhikari, B., 2015. Drying of shiitake mushroom by combining freeze-drying and mid-infrared radiation. Food and Bioproducts Processing, 94, 507-517.
Zielinska, M., Markowski, M., 2007. Drying behavior of carrots dried in a spout–fluidized bed dryer. *Drying Technology*, 25(1), 261-270.

نشریه پژوهشهای علوم و صنایع غذایی ایران
جلد 12، شماره 6، بهمن - اسفند 1395، ص. 766-758

Iranian Food Science and Technology Research Journal
Vol. 12, No. 6, Feb. Mrch. 2017, p. 758-766

ارزیابی تجربی و مدل سازی انتقال جرم طی خشک کردن مادون قرمز به

محمدامین مهرنیا[1]- آیگین باشتی[2]- فخرالدین صالحی[3]

تاریخ دریافت: 1395/10/21
تاریخ پذیرش: 1396/02/18

چکیده

در این تحقیق بررسی تجربی و مدل سازی انتقال جرم در طی خشک کردن مادون قرمز به مورد مطالعه قرار گرفت. در بخش تجربی، اثرات شرایط مختلف خشک کردن مانند توان پرتودهی مادن قرمز (W 375-150) و فاصله منبع مادون قرمز (cm 15-5) بر روی ویژگی های خشک کردن به مورد ارزیابی قرار گرفت. هر دوی توان پرتودهی و فاصله بر روی زمان خشک کردن قطعات به تاثیر گذار بودند. نسبت های رطوبت بر روی 8 مدل ریاضی مختلف با استفاده از آنالیز رگرسیون غیر خطی برازانده شد. نتایج رگرسیون نشان داد که مدل رگرسیونی به شکل رضایت بخشی رفتار خشک کردن را توصیف می کند. ضریب انتشار رطوبت موثر با افزایش توان در دامنه 1/15 تا $3/72\times 10^{-8}$ m^2/s افزایش یافت. افزایش توان مادن قرمز اثر منفی بر روی ΔE اثر منفی داشته و با افزایش توان پرتو دهی مقدار آن کاهش یافت. مقادیر کروما و هیو به ترتیب در دامنه های 43/8 تا 46/99 و °80/82 تا °86/14 قرار داشت.

واژه های کلیدی: ضریب انتشار موثر، پردازش تصویر، خشک کن مادن قرمز، به

1-استادیار، گروه علوم و صنایع غذایی، واحد شوشتر، دانشگاه آزاد اسلامی، شوشتر، ایران
2- استادیار، گروه شیمی، واحد شوشتر، دانشگاه آزاد اسلامی، شوشتر، ایران
3- استادیار، گروه علوم و صنایع غذایی، دانشگاه بوعلی سینا، همدان، ایران
(*- نویسنده مسئول : Email: mamehrnia@yahoo.com)